

Temperature-dependent thermal conductivity of porous silicon

This content has been downloaded from IOPscience. Please scroll down to see the full text.

1997 J. Phys. D: Appl. Phys. 30 2911

(<http://iopscience.iop.org/0022-3727/30/21/001>)

View [the table of contents for this issue](#), or go to the [journal homepage](#) for more

Download details:

IP Address: 142.51.1.212

This content was downloaded on 01/11/2013 at 21:49

Please note that [terms and conditions apply](#).

Temperature-dependent thermal conductivity of porous silicon

G Gesele[†], J Linsmeier^{†§}, V Drach[†], J Fricke[†] and R Arens-Fischer[‡]

[†] Physikalisches Institut der Universität Würzburg, Am Hubland, D-97074 Würzburg, Germany

[‡] I. Physikalisches Institut, RWTH Aachen, D-52056 Aachen, Germany

Received 19 May 1997

Abstract. The thermal conductivity λ_{PS} of electrochemically etched porous silicon (PS) layers was determined over a wide temperature range ($T = 35\text{--}320\text{ K}$) using the dynamic 3ω technique. Both the doping level of the silicon wafers (p and p⁺) and the porosity P of the porous layers ($P = 64\text{--}89\%$) were varied. The measured thermal conductivities were three to five orders of magnitude smaller than the values for bulk silicon. Furthermore, they increase with increasing the wafer doping level and with decreasing the porosity P of the layers. For all investigated PS layers the thermal conductivity increases with temperature. The results are discussed in terms of a simple model for heat conduction in PS based on the phonon diffusion model.

1. Introduction

Since the discovery of visible photoluminescence in porous silicon (PS) at room temperature [1] this material has been investigated extensively. With respect to possible applications in optoelectronics, the structural and chemical properties of PS and their influence on the colour, efficiency and stability of the luminescence have been studied in detail (see e.g. [2]).

Moreover, for optoelectronic applications the thermal properties of PS play an important role. In light emitting devices (LEDs) or photodiodes, heat is generated due to electrical losses or photon absorption. In order to optimize the thermal management of such a device the thermal conductivity of the PS layer has to be known.

The thermal conductivity of PS is also of interest in other applications. In applied microsystem technology, e.g. in thermal infrared or gas sensors, oxidized PS serves as a thermal insulator [3].

Up to now, only the room-temperature thermal conductivity of porous silicon has been determined. Using a dynamic measurement method, Lang and co-workers [3] determined the thermal conductivity of PS at room temperature on differently n- and p-doped silicon before and after thermal oxidation. Cruz-Orea and co-workers [4] measured the thermal conductivity of spark-processed PS layers by the photoacoustic technique.

We have determined the thermal conductivity λ_{PS} of electrochemically prepared PS layers over a wide temperature range ($T = 35\text{--}320\text{ K}$) using a dynamic method—the so-called 3ω technique [5–7]. Additionally,

we describe here a simple model for the heat conduction in PS which allows one to predict the temperature behaviour of the thermal conductivity of PS.

2. Experimental details

PS layers were formed by electrochemical etching [8] of (100)-oriented single-crystal boron-doped p⁺- and p-type silicon wafers with a resistivity $0.01\ \Omega\text{ cm}$ and $0.2\ \Omega\text{ cm}$ respectively. The electrolyte consisted of 48 wt% HF and pure ethanol in a volume ratio of 1:1. The porosities of the investigated samples were $P = 64, 71, 79$ and 89% and their thicknesses were between $d = 21\ \mu\text{m}$ and $d = 46\ \mu\text{m}$ (see table 1). Both P and d were determined gravimetrically [8] on separate samples. In order to avoid partial destruction due to capillary forces during drying in air, the highly porous layers with $P = 79\%$ and 89% were dried supercritically in CO₂ [9].

Layers prepared on lightly doped p-silicon show an isotropic structure [10, 11] with smaller inhomogeneities compared to the layers prepared on heavily doped p⁺-silicon. Moreover, in the latter case structural anisotropy can be observed, i.e. long voids running perpendicularly to the surface with small side branches [11].

The thermal conductivity of freshly prepared PS layers was determined using the 3ω technique [5]. A narrow metal line, prepared by vapour deposition, served as both the heater and the thermometer for the experiment. We used an approximately 100 nm thick and $22\ \mu\text{m}$ wide layer of Ag directly deposited onto the porous surface (see figure 1). The metal line was heated by applying an oscillating current with frequency ω yielding Joule heating

§ To whom correspondence should be addressed.

Table 1. Parameters of the investigated PS layers. The porosities P and layer thicknesses d were determined gravimetrically. The mean crystallite sizes d_k of the silicon structures in the porous layers were determined by small angle x-ray scattering (SAXS) using a two-phase media model. The penetration depth corresponds to the frequency range of the thermal wave which has to satisfy equation (4).

Doping level	Porosity P (%)	Thickness d (μm)	Penetration depth ℓ_0 (μm)	Crystallite size d_k (nm)
p	71 ± 2	31 ± 3	16–25	2.0 ± 0.3
p	71 ± 2	46 ± 6	17–29	2.0 ± 0.3
p	64 ± 2	31 ± 4	13–22	1.7 ± 0.5
p	79 ± 2	31 ± 4	16–25	2.7 ± 0.3
p	89 ± 2	35 ± 4	17–32	4.5 ± 0.6
p ⁺	64 ± 2	21 ± 3	13–18	9.0 ± 3.0

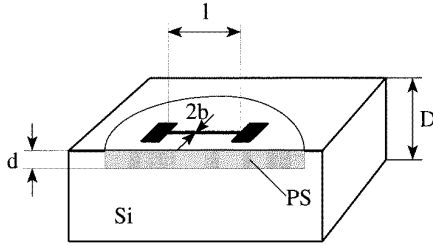


Figure 1. Schematic diagram of cross section of a porous silicon (PS) layer on a Si wafer of thicknesses d ($\approx 30 \mu\text{m}$) and D ($500 \mu\text{m}$) respectively. An approximately 100 nm thick Ag line of length l ($\approx 5 \text{ mm}$) and width $2b$ ($\approx 22 \mu\text{m}$) with contact pads was deposited directly onto the porous layer.

and hence temperature oscillations in the metal line at frequency 2ω . These temperature oscillations at 2ω were measured by voltage oscillations at the third harmonic 3ω caused by the temperature-dependent resistance of the metal line. In order to detect this voltage component at frequency 3ω we used a lock-in amplifier integrated into a Wheatstone bridge. The measurements were performed at temperatures between 35 K and 320 K in an evacuated ($p \approx 10^{-4}$ mbar) sample chamber in order to suppress convection and gaseous conduction.

Neglecting radiative heat transport, the heat conduction in the solid state is described by the differential equation of heat conduction [12]. The approximated solution of this equation for a given metal line of width $2b$ and length l (see figure 1) yields the following formula correlating the complex amplitude δT of the temperature oscillations in the metal line and the thermal conductivity λ of the underlying material [5]:

$$\delta T = \frac{P_0}{\pi l \lambda} \left[-\frac{1}{2} \ln \left(\omega \frac{1}{H_z} \right) + \frac{1}{2} \ln \left(\frac{a}{b^2} \frac{1}{H_z} \right) + \text{constant} - i \frac{\pi}{4} \right] \quad (1)$$

where P_0 denotes the amplitude of the heating power and a is the thermal diffusivity

$$a = \lambda / \rho c_p \quad (2)$$

of the material with density ρ and mass-specific heat capacity c_p . According to equation (1) the slope of a $\text{Re}(\delta T) - \ln \omega$ plot allows direct determination of λ .

The penetration depth ℓ_0 of the thermal wave within the material depends on the frequency ω of the heating current

$$\ell_0 = \sqrt{\frac{\lambda}{2\rho c_p \omega}}. \quad (3)$$

Generally, equation (1) only holds for an isotropic and homogeneous material. This is only true for the investigated PS layers on p-silicon; the layers on p⁺-silicon do not comply exactly with this assumption (see section 4). Moreover, the penetration depth ℓ_0 has to be much larger than the width $2b$ of the metal line ($\ell_0 \gg 2b$) and therefore the sample thickness L has to fulfil the condition $L \gg 2b$.

In our case, however, a typical PS sample consisted of a PS layer with a typical thickness d of about $30 \mu\text{m}$ on a bulk silicon layer with thickness D of about $500 \mu\text{m}$. The typical width $2b$ of the evaporated metal lines was $22 \mu\text{m}$. Nevertheless, numerical calculations have shown that the thermal conductivity of a layer can be determined by equation (1) as long as the penetration depth is larger than half the width of the metal line, $\ell_0 > b$ [13], and smaller than the thickness d of the layer, $\ell_0 < d$ [14].

Due to equation (3) λ can be determined reliably only within a certain frequency range in the $\text{Re}(\delta T) - \ln \omega$ plot. From equations (2) and (3) we get

$$\frac{1}{d} \sqrt{\frac{a}{2}} < \omega < \frac{1}{b} \sqrt{\frac{a}{2}} \quad (4)$$

for the possible frequency range for evaluation using equation (1).

Figure 2 shows a typical measured $\text{Re}(\delta T) - \ln \omega$ plot. The full dots within $\omega/2\pi = 22$ to 50 Hz correspond to a penetration depth $\ell_0 = 16$ to $25 \mu\text{m}$ and can be used for a linear fit. According to equation (1) the thermal conductivity λ_{PS} of the PS layer can be calculated from the slope of this line. The open circles deviate from the constant slope. For $\omega/2\pi > 50 \text{ Hz}$ the penetration depth ℓ_0 is too small, yielding an enlargement of δT . For $\omega/2\pi < 22 \text{ Hz}$ ℓ_0 is too large, resulting in smaller values of δT ; in this case the thermal oscillations reach the Si substrate so that its high thermal conductivity renders δT too small. In both cases a δT dependence with a smaller slope is caused, corresponding to larger values of λ_{PS} .

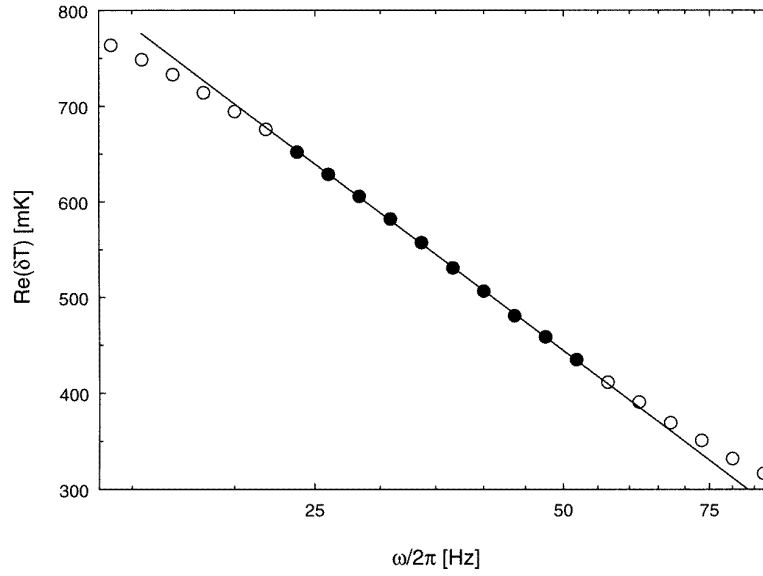


Figure 2. Real part $\text{Re}(\delta T)$ of the amplitude δT of the temperature oscillation within the metal heater versus the logarithm of the frequency ω of the heating current. The thickness of the PS layer is $31 \mu\text{m}$, the width of the metal line is $22 \mu\text{m}$. The full dots (\bullet) within $\omega/2\pi = 22$ to 50 Hz correspond to a penetration depth $\ell_0 = 16$ to $25 \mu\text{m}$. They were used for the calculation of λ_{PS} according to equation (1), (— fitted line).

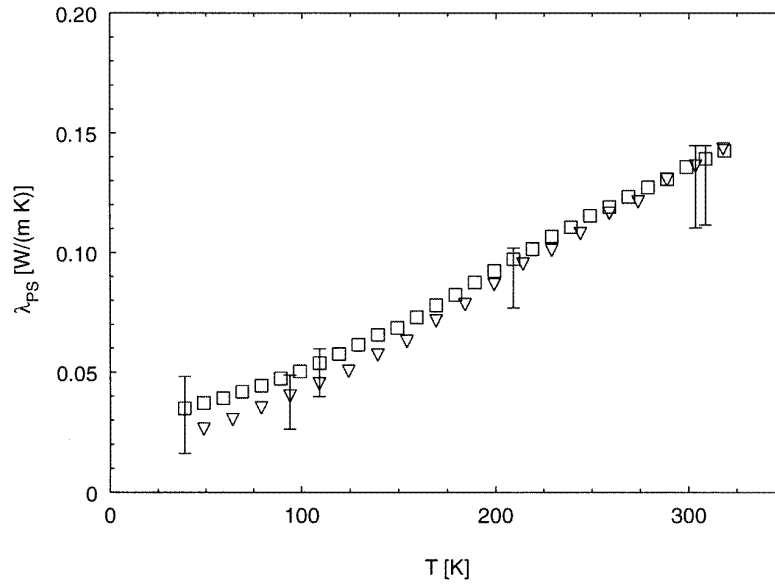


Figure 3. Thermal conductivity λ_{PS} of PS layers on p-silicon versus temperature T for porosity $P = 71\%$ and two different layer thicknesses $d = 31 \mu\text{m}$ (\square) and $46 \mu\text{m}$ (∇).

3. Theory

We now present a simple model for the thermal conductivity λ_{PS} of porous silicon.

In analogy with other transport properties, like electrical conductivity, the effective thermal conductivity λ_{eff} of a porous medium consisting of a solid phase with thermal conductivity λ_s and voids with $\lambda_v \approx 0$ can be described by [15–16]:

$$\lambda_{eff} = f g_0 \lambda_s \quad (5)$$

where $f = (1 - P)$ denotes the volume fraction of the solid phase within the porous medium of porosity P . The percolation strength g_0 depends on the microtopology of the porous system and can be interpreted as the fraction of the solid phase which is interconnected and thus contributes to the thermal conduction. The microtopology of PS is well approximated by the Looyenga effective medium model [17] where a fixed correlation between g_0 and the volume

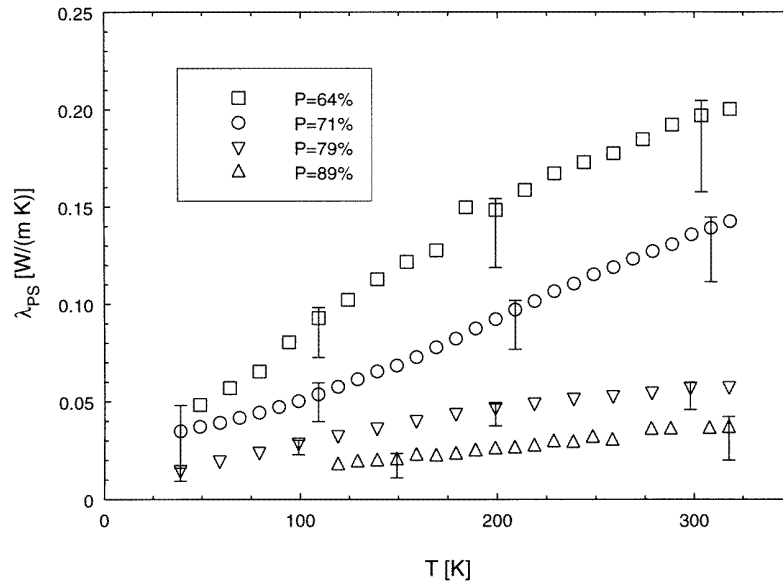


Figure 4. Thermal conductivity λ_{PS} for PS layers of thickness $d \approx 31 \mu\text{m}$ and different porosities $P = 64, 71, 79$ and 89% on p-silicon.

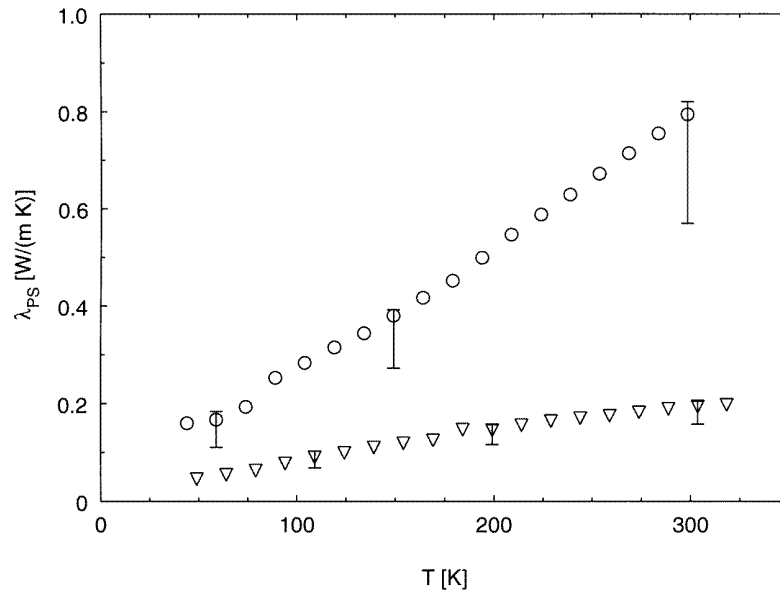


Figure 5. Thermal conductivity λ_{PS} of PS layers for different substrate doping levels: p⁺- (○) and p-type (▽) silicon for $P = 64\%$.

fraction f of the solid phase is given [15, 16]

$$g_0 = f^2. \quad (6)$$

In semiconductors—even in the degenerate case—the contribution of the electrons to the thermal conductivity of the bulk material is small compared to that of the phonons [18], e.g. for our p⁺-silicon wafers the ratio of the electronic to the phononic contribution of the *bulk* material is about 10^{-4} . In our model this small contribution should scale down with f in the same way as the phononic contribution (equations (5) and (6)). Consequently the electronic contribution to the *effective* thermal conductivity of the porous

system remains small compared to the phononic contribution and can hence be neglected in further discussions.

Based on the phenomenologic phonon diffusion model the thermal conductivity of bulk silicon λ_s is given by

$$\lambda_s = \frac{1}{3} \rho c_v v \ell \quad (7)$$

where ρ , c_v , v and ℓ are the density, mass-specific heat capacity, sound velocity and mean free path of the phonons in silicon respectively. At high temperatures ($T \gg \Theta_{D,Si} = 625 \text{ K}$) the value of c_v is a constant and λ_s is dominated by the mean free path ℓ of the phonons.

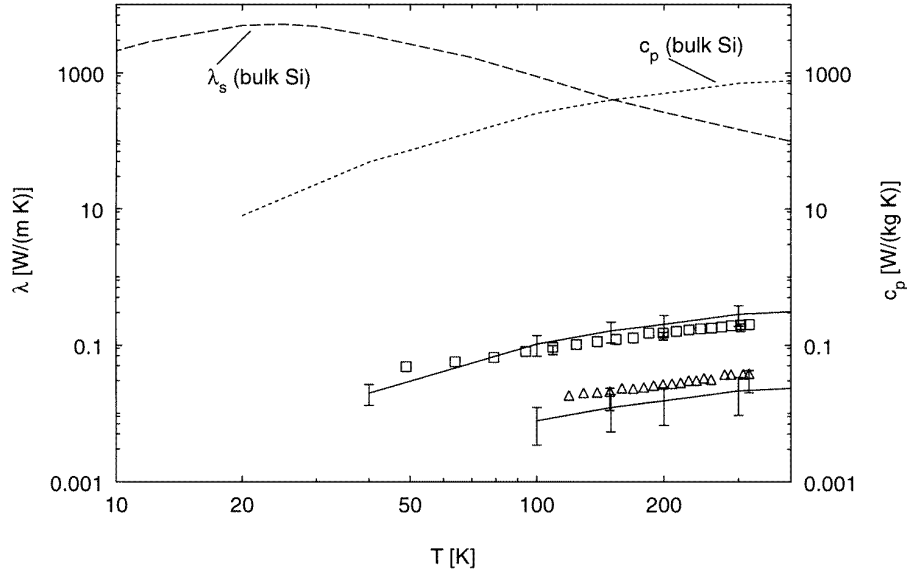


Figure 6. Comparison of the experimental values of λ_{PS} on p-silicon for $P = 64\%$ (\square) and 89% (\triangle) with the theoretical model (—) and the bulk silicon thermal conductivity λ_s (---). The specific heat capacity c_p (·····) of bulk silicon is also plotted.

For decreasing temperatures ℓ increases until it is limited by the crystal dimensions and becomes a constant. In this temperature region the thermal conductivity is dominated by the temperature dependence of the specific heat capacity c_v [19].

The mean free path ℓ of phonons in silicon at room temperature is approximately 40 nm which is significantly larger than the mean size d_k of the silicon crystallites in the investigated PS layers with typical values of about 3 nm [20]. In analogy to the limitation of ℓ by the crystal dimensions mentioned above we assume that in PS layers the mean free path of phonons in the silicon crystallites is limited by the mean size of the crystallites so that ℓ in equation (7) can be substituted by d_k . Together with equation (5) and (6) we obtain for $d_k < \ell$:

$$\lambda_{PS} = \lambda_{eff} \approx f g_0 \frac{1}{3} \rho c_v v d_k = \frac{1}{3} f^3 \rho c_v v d_k \quad (8)$$

with the bulk silicon values $\rho = 2330 \text{ kg m}^{-3}$, $v = 6562 \text{ m s}^{-1}$ and $c_v \approx c_p$. The mean crystallite size d_k of silicon structures (see table 1) in the porous layer was determined by small angle x-ray scattering (SAXS) [20] using a two-phase media model for a non-particulate system [21].

As in the case of bulk silicon at low temperatures, the temperature dependence of λ_{PS} within the measured temperature region between 35 and 320 K is dominated by the temperature dependence of $c_p = c_p(T)$.

4. Results and discussion

First we present the results for PS layers on lightly doped p-type silicon wafers. In figure 3 the thermal conductivity λ_{PS} of PS layers of porosity $P = 71\%$ and different thicknesses d is plotted versus temperature

T . As expected, the layer thickness does not influence the determination of λ_{PS} within the uncertainties of measurement and evaluation. The measured thermal conductivities λ_{PS} between 300 K and 35 K are about three to five orders of magnitude smaller than those of bulk silicon with $\lambda_{Si,300 \text{ K}} = 148 \text{ W m}^{-1} \text{ K}^{-1}$ and $\lambda_{Si,35 \text{ K}} = 4090 \text{ W m}^{-1} \text{ K}^{-1}$, respectively [22]. Within the measured temperature range the thermal conductivity of porous silicon increases monotonically with temperature.

Figure 4 shows λ_{PS} versus temperature for different porosities $P = 64\text{--}89\%$. Obviously, λ_{PS} decreases dramatically with increasing porosity P for all temperatures studied.

These results can be explained by our model. According to equation (8), the effective thermal conductivity of PS layers is correlated with the volume fraction $f = 1 - P$ of the silicon phase and the mean size of the silicon crystallites d_k . As f is of the order of 10^{-1} the dependence on f^3 can explain the facts that λ_{PS} is several orders of magnitude smaller than λ_s of bulk Si and that λ_{PS} varies dramatically with the porosity of the PS layers.

In order to study the influence of the doping level on the thermal conductivity of PS we prepared layers of porosity $P = 64\%$ on differently doped, p- and p⁺-type, silicon. Figure 5 shows the measured thermal conductivities. Although the porosities are equal (and the different layer thicknesses do not influence the determination of λ_{PS} significantly) the measured thermal conductivity of PS on the heavily doped p⁺-silicon substrate is about three to four times higher than that of the PS layer on the lightly doped p-silicon.

This result can be explained by the microstructure of PS layers on differently doped silicon substrates (see section 2). Due to the larger crystallites in PS prepared on p⁺-silicon, according to equation (8) λ_{PS} is expected to be larger than

for layers prepared on p-silicon. Additionally, because of the structural anisotropy the thermal conductivity perpendicular to the surface is expected to be different to that parallel the surface. However, by the applied 3ω technique the geometric average of the thermal conductivities for these two directions can be measured (see [12] or [14]). Because our model does not account for structural anisotropy, a quantitative prediction is difficult. Nevertheless, the measured value is in the order of the theoretically predicted one. With the mean crystallite size d_k (see table 1) and a percolation strength g_0 approximately equal to that of PS prepared on lightly doped p-silicon we get $\lambda_{PS} \approx 1.5 \pm 0.6 \text{ W m}^{-1} \text{ K}^{-1}$ at $T = 300 \text{ K}$ compared with the measured value of $0.8 \pm 0.1 \text{ W m}^{-1} \text{ K}^{-1}$.

In figure 6 the temperature dependence of λ_{PS} is compared with the model calculations for the samples of p-silicon with porosity $P = 64\%$ and 89% . Additionally, the thermal conductivity of a typical crystalline bulk silicon sample is plotted [22]. Within the error of measurement and evaluation the model calculations are in good agreement with the measured values. The different temperature behaviour of bulk and porous silicon is obvious: while λ_s of bulk Si increases with decreasing temperature, λ_{PS} decreases. The latter result is consistent with the assumption that the mean free path of phonons in the PS layers is restricted by the crystallite dimensions and hence the temperature dependence of λ_{PS} is determined by the heat capacity c_p (also plotted in figure 6).

5. Conclusion

In this work the thermal conductivity λ_{PS} of porous silicon layers was measured over a wide temperature range using the 3ω technique. For layers on p-doped silicon with porosities $P = 64\text{--}89\%$ the thermal conductivity λ_{PS} decreases with increasing P . The PS layer on p⁺-doped silicon with $P = 64\%$ shows a thermal conductivity which is about three to four times higher than that of PS on p-doped silicon. For all the investigated samples the thermal conductivity increases with temperature. The dependence of λ_{PS} on porosity, wafer doping level and temperature can be described in terms of a simple model for heat conduction in PS based on the phonon diffusion model.

Acknowledgment

This work was supported by the Deutsche Forschungsgemeinschaft (DFG), Bonn.

References

- [1] Canham L T 1990 *Appl. Phys. Lett.* **57** 1046
- [2] Vial J-C and Derrien J (ed) 1995 *Porous Silicon Science and Technology* (Berlin: Springer)
- [3] Lang W, Drost A, Steiner P and Sandmaier H 1995 *Mater. Res. Soc. Symp. Proc.* **358** 561
- [4] Cruz-Orea A, Delgadillo I, Vargas H, Gudino-Martinez A, Vazquez-Lopez C, Calderon A and Alvarado-Gil J J 1996 *J. Appl. Phys.* **79** 8951
- [5] Cahill D G 1990 *Rev. Sci. Instrum.* **61** 802
- [6] Cahill D G, Fischer M E, Klitsner T, Schwartz E T and Pohl R O 1989 *J. Vac. Sci. Technol. A* **7** 1259
- [7] Frank R, Drach V and Fricke J 1993 *Rev. Sci. Instrum.* **64** 760
- [8] Halimaoui A 1995 *Porous Silicon Science and Technology* ed J-C Vial and J Derrien (Berlin: Springer) p 33
- [9] Frohnhoff S, Arens-Fischer R, Heinrich T, Fricke J, Arntzen M and Theiss W 1995 *Thin Solid Films* **225** 115
- [10] Smith R L and Collins S D 1992 *J. Appl. Phys.* **71** R1–21
- [11] Naudon A, Goudeau P and Vezin V 1995 *Porous Silicon Science and Technology* ed J-C Vial and J Derrien (Berlin: Springer) p 255
- [12] Carslaw H S and Jaeger J C 1959 *Conduction of Heat in Solids* 2nd edn (Oxford: Clarendon)
- [13] Moon I K, Jeong Y H and Kwun S I 1996 *Rev. Sci. Instrum.* **67** 29
- [14] Frank R 1995 *PhD Thesis* Universität Würzburg
- [15] Theiß W 1989 *PhD Thesis* RWTH Aachen p 77, 96
- [16] Sturm J, Grosse P and Theiß W 1991 *Z. Phys. B–Condens. Matter* **83** 361
- [17] Looyenga H 1965 *Physica* **31** 401
- [18] Weißmantel Ch and Hamann C 1980 *Grundlagen der Festkörperphysik* (Berlin: Springer) p 419
- [19] Ashcroft N W and Mermin N D 1987 *Solid State Physics* (Philadelphia, PA: Saunders College)
- [20] Linsmeier J, Pröbstle H, Emmerling A and Fricke J 1996 *Annual Report of the HASYLAB/DESY* pt 1 (Hamburg) pp 503–4
- [21] Porod G 1982 *Small Angle X-ray Scattering* ed O Glatter and O Kratky (London: Academic) pp 17–51
- [22] Touloukian Y S, Powell R W, Ho C Y and Klemens P G 1970 *Thermophysical Properties of Matter* vol 1, pt 1 (New York: IFI/Plenum) p 339